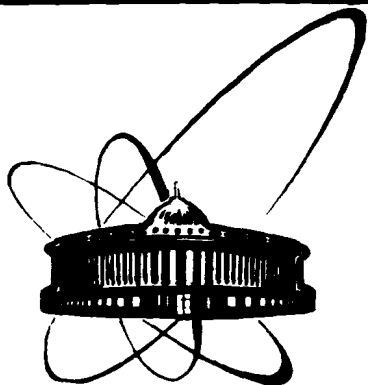


89-809



ОБЪЕДИНЕННЫЙ
ИНСТИТУТ
ЯДЕРНЫХ
ИССЛЕДОВАНИЙ
ДУБНА

A 55

E7-89-809

A. N. Andreyev, D. D. Bogdanov, V. I. Chepigin,
A. V. Yeremin, A. P. Kabachenko, Yu. A. Muzichka,
O. A. Orlova, B. I. Pustynnik, Sh. Sharo,
G. M. Ter-Akopian

PRODUCTION CROSS SECTIONS
OF NEUTRON DEFICIENT ISOTOPES
OF At AND Po FROM NUCLEAR REACTIONS

$^{165}\text{Ho} + ^{40}\text{Ar}$, $^{159}\text{Tb} + ^{40}\text{Ca}$ AND $^{181}\text{Ta} + ^{24}\text{Mg}$

Submitted to "Ядерная физика"

1989

2. EXPERIMENTAL SET-UP

1. INTRODUCTION

The interest in the investigations of the cross sections of complete fusion reaction products with $85 \leq Z \leq 95$ in heavy ion nuclear reactions is evoked by the fact that this region is an intermediate one with respect to fission. In this region of nuclei the liquid drop fission barrier decreases from ≈ 10 MeV for neutron deficient isotopes of Po - At to ≈ 2.5 MeV for the Pu-Am neutron deficient isotopes. Usually this fact is used as an explanation for the sharp decrease of cross sections for xn evaporation channels: from tens of millibarns for Po - At to less than one microbarn for U-Pa [1-3]. Nevertheless, in the region of neutron deficient isotopes the decrease of cross sections for the xn channels may be caused by an increase of the contribution from reactions involving the evaporation of charged particles to the total cross section of complete fusion reactions. This trend will become stronger with the increasing neutron deficit of the product nuclei. The incorrect consideration of this effect in theoretical calculations can substantially influence the interpretation of experimental results and, consequently, the information about the effect of fission on the cross sections of the complete fusion reaction products. The isotopes of At and Po are the most suitable objects in this region for the investigation of the behavior of the cross sections of xn and pxn type reactions as a function of the neutron deficit. First, by using ^{40}Ar and ^{40}Ca ion beams we can obtain data over the wide ranges of mass numbers, $173 \leq A \leq 202$, and excitation energies. Second, as the liquid drop fission barrier is high enough in these nuclei, we can assume that its decrease with decreasing mass number will not effect the cross sections strongly. The above given considerations were a motivation for the present work.

To carry out the experiments the U-400 cyclotron of the Laboratory of Nuclear Reactions, JINR Dubna was used. The projectile beams were as follows: ^{40}Ca (228 MeV), ^{40}Ar (217, 250, and 293 MeV), and ^{24}Mg (141 and 172 MeV). The beam intensities, passing through targets (12 mm in diameter) were $(3-6) \times 10^{11}$ particles/sec at an energy spread (1-1.5)%. A schematic view of the experimental set-up is shown in fig.1. The beam energy was changed in 3 - 6 MeV steps using Al and Ti degraders. The energy of the beam after passing through degraders was controlled by measuring the energy of ions, scattered in a thin ($200 \mu\text{g}/\text{cm}^2$) foil at 30° . For this purpose a surface barrier detector was used. In front of one half of the detector surface a $3 \mu\text{m}$ thick Ti foil was placed to provide the possibility of controlling the possible admixture of ^{40}Ar in the ^{40}Ca beam. Such a control can be fulfilled because of the difference between the electronic stopping powers of these ions. The Ho, Tb, and Dy oxide targets had thicknesses of $350 \mu\text{g}/\text{cm}^2$, $400 \mu\text{g}/\text{cm}^2$, and $500 \mu\text{g}/\text{cm}^2$, respectively. They were prepared by deposition onto a Ti backing $1.35 \mu\text{g}/\text{cm}^2$ thick. As a Ta target a $0.8 \text{ mg}/\text{cm}^2$ thick foil was

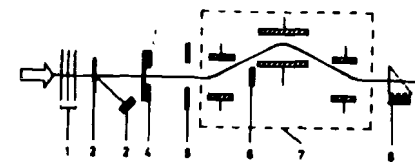
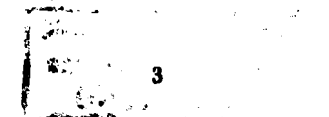


Fig.1 Block diagram of the experimental setup : 1 - degraders, 2 - Au - scatterer; 3 - detector to monitor beam energy; 4 - target; 5 - input diaphragm; 6 - Faraday cup; 7 - separator; 8 - time-of-flight detectors; 9 - semiconductor detector.



used. The target thickness was determined by weighing with an accuracy better than 10%. The composition of target material was controlled by roentgen-fluorescence analysis.

To separate the complete fusion reaction products from the projectile beam and from transfer reaction products the kinematic separator VASSILISSA [4,5] was used. The reaction products were separated according to their electric rigidity and the complete fusion reaction products were focused in a detector system 12 m far from the target.

The detector system consisted of two time-of-flight detectors and the array of seven surface barrier detectors. The energy resolution of the cooled detectors was 30 - 40 keV (FWHM). All detectors had separate data tracks to determine the energy and time-of-flight of evaporation residues, the time of their arrival in a detector, the energy and time of the consequent α -decays of all nuclei implanted into a detector.

The transport efficiency of the separator was measured in all experiments. For this purpose an Al catcher (1.8 mg/cm^2) was placed behind the target. The catcher was exposed for 15 min and then, for ≈ 30 sec, was removed to a Si(Au) detector situated inside the target chamber. During the following 15 min interval the decay curves of the activity implanted into the catcher were measured. Analogous measurements were carried out with the detectors placed in the focal plane of the separator. The comparison of the data obtained from the catcher and in the focal plane of the separator allowed us to determine the transport efficiency with an accuracy of $\pm 25\%$ in the case of nuclei having half lives ≥ 1 min. In those cases, where experiments were done with a ^{40}Ca projectile beam, the transport efficiency was determined using a reaction of $\text{Dy} + ^{40}\text{Ar}$. The ^{40}Ar beam was used before and after each experiment with a ^{40}Ca beam.

3. EXPERIMENTAL RESULTS

The nuclei observed in our experiments, were identified according to their α -transition energies and the half lives of long-lived activities. As the α -transition energies of Po and At isotopes are well known for the given mass region, there are no problems with the identification of nuclei. The relative line intensities, which are necessary for cross section determination, were taken from ref.[6]. The cross section values, obtained in our experiments are given in tables 1, 2, and 3. The values of excitation energies were calculated on the basis of the projectile beam energies at the target output. Energy losses in the targets and backings were calculated using tabulated values from ref.[7].

Tab.1. Excitation functions for the xn and pxn evaporation channels measured in the $^{165}\text{Ho} + ^{40}\text{Ar}$ reaction.

| E* MeV | Cross-section (μbarn) | | | | |
|-----------|------------------------------------|------|-----|------|------|
| | 5n | 6n | 7n | p,5n | p,6n |
| 54.0 | 2430 | | | | |
| 57.5 | 9300 | | | | |
| 59.5 | 8250 | 100 | | 100 | |
| 62.0 | 11500 | 460 | | 460 | |
| 65.0 | 8800 | 850 | | 320 | |
| 69.5 | 4650 | 1170 | | 550 | 90 |
| 72.5 | 2600 | 1930 | | 650 | 75 |
| 73.5 | 1700 | 1620 | 35 | 710 | 105 |
| 76.0 | 1250 | 1950 | 100 | 1340 | 250 |
| 79.5 | 350 | 800 | 300 | 910 | 620 |
| 82.5 | 210 | 320 | 350 | 600 | 750 |
| 89.0 | | 100 | 370 | 250 | 1050 |
| 93.5 | | 20 | 160 | 250 | 712 |
| 99.0 | | 28 | 150 | 70 | 475 |
| 103.5 | | | 35 | 60 | 260 |
| 107.0 | | 10 | 56 | 31 | 256 |
| 113.5 | | | 17 | 15 | 81 |
| 119.0 | | | 9 | | 24 |

Tab.1a. Excitation functions for the xn and pxn evaporation channels measured in the $^{165}\text{Ho} + ^{40}\text{Ar}$ reaction.

| E* MeV | Cross-section (μbarn) | | | | |
|-----------|------------------------------------|-----|------|-----|-----|
| | 8n | 9n | p7n | p8n | p9n |
| 82.5 | | | 100 | | |
| 89.0 | 15 | | 410 | 15 | |
| 93.5 | 35 | | 1000 | 30 | |
| 99.0 | 28 | | 600 | 84 | |
| 103.5 | 25 | 1.0 | 1000 | 150 | |
| 107.0 | 31 | 1.4 | 790 | 180 | |
| 113.5 | 16 | 3.0 | 560 | 345 | 19 |
| 119.0 | 4 | 3.5 | 220 | 330 | 54 |
| 125.0 | 1.5 | 1.7 | 90 | 230 | 90 |
| 131.0 | 0.8 | 1.0 | 36 | 140 | 120 |
| 137.5 | | | | 56 | 72 |

Tab.2. Excitation functions for the xn and pxn evaporation channels measured in the $^{181}\text{Ta} + ^{24}\text{Mg}$ reaction.

| E* MeV | Cross-section (μbarn) | | | | | | | |
|-----------|------------------------------------|------|-----|----|------|------|------|-----|
| | 5n | 6n | 7n | 8n | p5n | p6n | p7n | p8n |
| 55.2 | 24300 | 27 | | | 22 | | | |
| 64.0 | 29700 | 1980 | | | 900 | | | |
| 70.2 | 8100 | 4400 | 60 | | 2200 | 120 | | |
| 71.8 | 3300 | 3800 | 293 | | 2900 | 330 | | |
| 75.5 | 1720 | 2900 | 650 | | 2900 | 740 | | |
| 84.3 | 150 | 540 | 850 | 7 | 1100 | 1540 | 181 | 25 |
| 94.0 | | 35 | 270 | 50 | 160 | 1000 | 1100 | 58 |
| 98.5 | | 44 | 210 | 54 | 160 | 1100 | 1200 | 55 |
| 102.9 | | 12 | 77 | 43 | 54 | 450 | 1350 | 250 |

The Q-values were calculated using a table of masses [8]. The statistical error for most of the results is less than 5%, and the accuracy of the obtained cross section values is determined by

Tab.3. Excitation functions for the pxn and α xn evaporation channels measured in the $^{159}\text{Tb} + ^{40}\text{Ca}$ reaction.

| E* MeV | Cross-section (μbarn) | | | | | |
|-----------|------------------------------------|-----|-----|-----|-------------|-------------|
| | p2n | p3n | p4n | p5n | α 2n | α 4n |
| 51.6 | 23 | 41 | 0.5 | | 5000 | |
| 56.4 | 19 | 110 | 4 | | <300 | |
| 59.6 | 14 | 102 | 15 | | | 75 |
| 65.2 | | 40 | 42 | 0.3 | | 190 |
| 69.2 | < 2.5 | 30 | 89 | 3.0 | | 650 |

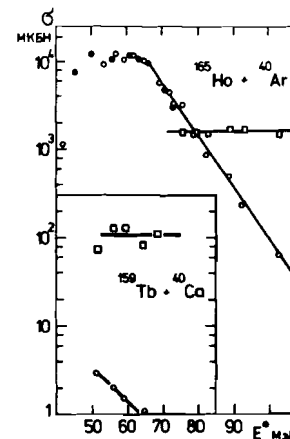


Fig.2. Total cross sections of the xn and pxn channels in the reactions $\text{Ho} + ^{40}\text{Ar}$ and $\text{Tb} + ^{40}\text{Ca}$, as functions of excitation energies. The marks o, \square and \bullet correspond to the xn, pxn and xn [ref.9] channels, respectively.

that of the separator's transport efficiency measurements, by the target thickness and homogeneity, and by the beam intensity. The control of the reproducibility of the obtained results has showed that the relative production rates of individual isotopes are reproduced with an accuracy of $\pm 20\%$ and the absolute cross section values with an accuracy of $\pm 40\%$. In fig.2 a comparison is made

between our experimental results and the results given in ref. [9]. We can see a very good agreement between these two works in the overlapping region of excitation energies. In fig.3 the behavior of excitation functions for the individual xn and pxn evaporation channels is shown for the $^{181}\text{Ta}+^{24}\text{Mg}$ reaction. Analogous excitation functions for the $^{165}\text{Ho}+^{40}\text{Ar}$ reaction, leading to the same compound nucleus, ^{205}At , are in good agreement (in terms of their shape and place on the excitation energy axis) with those shown in fig.3. The cross section values for all investigated evaporation channels of the $\text{Ta}+^{24}\text{Mg}$ reaction are 2.5 ± 0.1 times larger than that for the $^{165}\text{Ho}+^{40}\text{Ar}$ reaction.

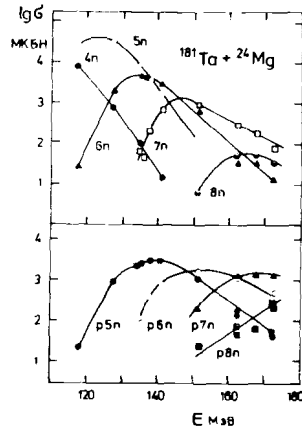


Fig.3. Excitation functions of the xn and pxn channels in the reaction $\text{Ta} + ^{24}\text{Mg}$.

4. ANALYSIS OF EXPERIMENTAL RESULTS

An analysis of experimental data on xn and pxn evaporation channel cross sections was based on the statistical model of the de-excitation process of compound nuclei. Calculations were carried out using a modified version of the ALICE program. To

describe the level density we used the relations of the Fermi gas model with the phenomenological consideration of shell effects in the level density parameter [11], i.e.

$$a_\nu(E) = \tilde{\alpha}_\nu (1 + [1 - \exp(-0.054E)](\Delta W_\nu/E)), \quad (1)$$

where E is the nuclear excitation energy, a_ν is the level density parameter for evaporation channels having an asymptotic value of $\tilde{\alpha}_\nu \cong A/10$, ΔW_ν is the shell correction for the nuclear mass after the evaporation of a particle ν (neutron, proton, or α -particle). In the fission channel $a_f = \tilde{\alpha}_f$.

We assumed that the fission barrier, of which the value has to be subtracted from the nuclear excitation energy (for the determination of the nuclear temperature) has the form

$$B_f(l) = CB_f^{\text{CPS}}(l) + \Delta B_f(Z, A) \quad (2)$$

where $B_f^{\text{CPS}}(l)$ is the fission barrier in the model of the rotating charged liquid droplet [12], C is a free parameter, $\Delta B_f(Z, A)$ is the shell correction for the compound nucleus fission barrier, equal to the difference between the liquid drop model and experimental values of the nuclear mass.

The cross section of the compound nucleus formation was calculated using the formula

$$\sigma_1 = \pi \lambda^2 \sum_{l=1}^{l_{\text{cr}}} \frac{1}{1 + \exp[2\pi(V_{B_1} - E_{\text{cm}})/\hbar\omega_1]}, \quad (3)$$

where V_{B_1} is the interaction barrier height, $\hbar\omega_1$ is the curvature of the barrier for the 1st wave. The potential parameters and the choice of l_{cr} were considered earlier [10]. The choice of these quantities is in principle very important for an attempt to describe the form of excitation functions. The aim of the calculations carried out in this work was the optimum description of the cross section maxima for xn and pxn reaction channels. More than 90% of cross section values in their maxima are achieved at $l \ll l_{\text{cr}}$ of the given reactions. For this reason the cross section

calculations for xn and pxn reaction channels were incorrect if the contribution of the following partial wave was $< 1\%$ of the given cross section. Three variants of calculations were made: a) $\Delta W_\nu = B_\nu = 0$, b) ΔB_f and corrections to the level density parameter are functions of the excitation energy and Z and A of all nuclei of the evaporation cascade, c) The quantity ΔB_f is independent of the excitation energy. At the same time, the level density parameter in the evaporation cascade of particles $a_\nu(E)$ is an energy dependent one [1, 10]. The parameter C (eq.2) and the ratio between the level density parameter in fission and in evaporation channels, $\tilde{\alpha}_f/\tilde{\alpha}_\nu$, were free parameters in all calculation variants. It should be noted that there was no necessity in using the $\tilde{\alpha}_f/\tilde{\alpha}_\nu$ values differing from 1 in the fitting the experimental and calculated cross section values for xn and pxn evaporation channels.

In fig.4 the dots indicate the experimental cross section values for the xn reaction products for the maximum value of the given excitation function of the $^{165}\text{Ho} + ^{40}\text{Ar}$ reaction. The

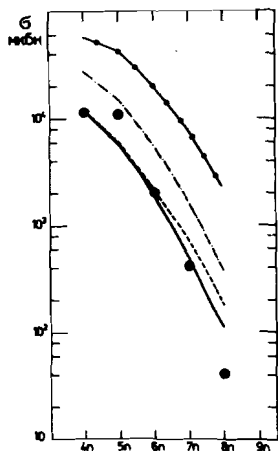


Fig.4. Comparison of the experimental and calculated values of the xn channel cross section for the reaction $\text{Ho} + ^{40}\text{Ar}$.

dash-dotted line is drawn through the calculated values of these quantities for $\Delta B_f = \Delta W_\nu = 0$, $a_f/a_\nu = 1$, and $C = 1$. In this variant of fitting the experimental and calculated values it was necessary to set $C = 0.9$. This value of C corresponds to a decrease in the fission barrier by about 1 MeV (the full line in fig.4). The results of calculations including shell corrections to the fission barriers for nuclei involved in the evaporation cascade, independent of the excitation energy, are represented in fig.4 with a circle-dashed line. If we use the shell corrections ΔB_f , which decrease at the same rate as the corrections of the level density parameter do with an increase in E^* , then we get a satisfactory agreement with experimental results (dotted line). In these calculations C and a_f/a_ν are equal to 1. An analogous picture is obtained also for the $^{181}\text{Ta} + ^{24}\text{Mg}$ reaction (fig.5).

In fig.6 the result obtained for the pxn evaporation channels in the $^{165}\text{Ho} + ^{40}\text{Ar}$ reaction is shown. In this case the abscissa axis gives the mass number of the Po isotopes, obtained

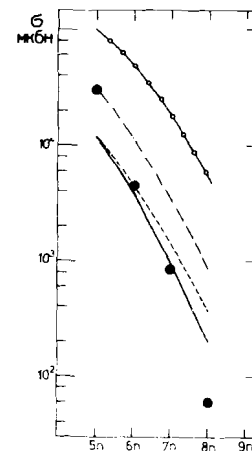


Fig.5. Comparison of the experimental and calculated values of the xn channel cross section for the reaction $\text{Ta} + ^{24}\text{Mg}$.

after the evaporation of one proton and x neutrons, rather than the number of neutrons in a cascade. In fig.6 small squares indicate the results for the $p2n$, $p3n$, and $p4n$ evaporation channels, obtained in the $^{159}\text{Tb} + ^{40}\text{Ca}$ reaction. The full lines represent the calculated results for both reactions for $\Delta B_f = \Delta W_v$

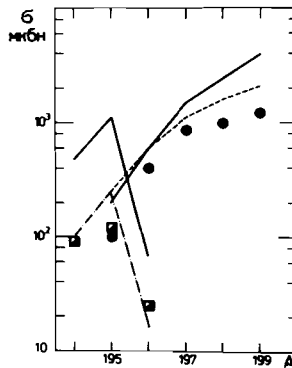


Fig.6. Comparison of the experimental and calculated values of the p_{xn} channel cross sections in the reactions $\text{Ho} + ^{40}\text{Ar}$ and $\text{Tb} + ^{40}\text{Ca}$.

$= 0$, $a_f/a_v = 1$, and $C = 0.9$. While this variant of calculations for the $^{165}\text{Ho} + ^{40}\text{Ar}$ reaction gives a satisfactory agreement with the experimental results, for the $^{159}\text{Tb} + ^{40}\text{Ca}$ reaction the calculated values lie above the experimental ones. To fit the experimental and calculated values for this reaction, the parameter C should be lowered to 0.8 (semicolon line). This result can be interpreted as an indication that for the strongly neutron deficient nuclei the rotating charged liquid drop model [12] gives overestimated values for the fission barrier.

5. CONCLUSIONS

In reactions with the heavy ions of ^{24}Mg , ^{40}Ar and ^{40}Ca the experimental values of cross sections were obtained for the xn

and p_{xn} evaporation channels up to $x = 9$ over a wide region of energies. To investigate the fusion - evaporation type reactions Po and At neutron deficient isotopes are very convenient. The de-excitation of the compound nuclei was analyzed using a statistical model. The statistical model, used to analyze the experimental cross section values of the xn and p_{xn} evaporation channels, is a phenomenological one. Therefore the unambiguous choice of basic parameters is of fundamental importance. If the nuclear masses and binding energies of nucleons and α -particles are calculated reliably and unambiguously enough, then in the choice of fission barrier parameters and level densities we can have certain freedom. Under the same assumption about the structure of the fission barriers and of the level density parameters, the excitation functions for fission reactions were analyzed earlier [13]. It is shown, in both cases, that a satisfactory agreement between experimental and calculated results can be achieved in two cases: a) In using $\tilde{a}_f/\tilde{a}_v \cong 1$ and $B_f(1) \cong (0.8-0.9)B_f^{\text{CPS}}(1)$, but without including shell effects; b) In including shell effects in the level density parameters and also in fission barriers.

At the same time, we see in this work, that with the increasing neutron deficit of the end product nuclei of evaporation cascades the agreement between experimental and calculated values is getting worse. Therefore a question arises about the choice of the isospin dependence parameter K , which is a part of the expression for the surface energy in the liquid drop model, $(E_s = a_s A^{2/3} [1 - K(\frac{N-Z}{N+Z})^2])$. Theoretical estimates of the value of this parameter in different works are very different, varying from $K = 1.78$ [14] (used in this work) to $K = 3.0$ in ref [15]. As we can see, it would be very interesting to continue the investigation of the evaporation end-products of compound nuclei - the very neutron deficient isotopes of $\text{At} - \text{Bi}$.

References

1. O.-C. Sahm et al. Nucl. Phys. A441 (1985) p. 316.
2. А.Н. Андреев и др., Ядерная физика, том 50, вып. 9, (1989), с. 819
3. H.W. Gaggeler et al. PSI-Bericht Nr. 29 (1989).
4. A.V. Yegemin et al. NIM A274 (1989) p. 528.
5. А.Н. Андреев и др. Краткие сообщения ОИЯИ № 3[29]-88 (1988) p. 33.
6. W. Westmeier, A. Merklin. Catalog of Alpha-Particles from Radioactive Decay. Karlsruhe (1985). Nr. 29-1.
7. R.L. Northcliff, R.F. Shilling. Nucl. Data Tables A7 (1970) p. 233
8. N. Zeldes et al. Mat. Fis. Scr. Dan. Vid. Selsk 3 (1967), Nr. 5.
9. D. Vermeulen et al. Z. Phys. A 318 (1984) p. 157.
10. Ю.А. Музычка, Б.И. Пустыльник. Препринт ОИЯИ, ДЗ-83-844, Дубна, 1983, с. 420.
11. А.В. Игнатюк и др. ЯФ, 21, (1975) с. 486.
12. S. Cohen, F. Plasil, W. Swiatecki. Ann. Phys., (1974) Nr. 82, p. 557
13. С.Д. Бейзин и др., Ядерная физика, 37, (1983), с. 809.
14. W.D. Myers, W.J. Swiatecki, Ark. Fysik, (1967), Nr. 36, p. 538.
15. H. J. Krappe, J.R. Nix, A. J. Sierk, Phys. Rev., C20, (1979), p. 992.

Received by Publishing Department
on December 6, 1989.

Андреев А.Н. и др. Е7-89-809
Сечения образования нейтронодефицитных изотопов
At и Po в реакциях $^{165}\text{Ho} + ^{40}\text{Ar}$, $^{159}\text{Tb} + ^{40}\text{Ca}$ и $^{181}\text{Ta} + ^{24}\text{Mg}$

Проведены эксперименты по измерению сечений (xn) и (p, xn)-каналов в реакциях $^{165}\text{Ho} + ^{40}\text{Ar}$, $^{181}\text{Ta} + ^{24}\text{Mg}$ и $^{159}\text{Tb} + ^{40}\text{Ca}$. Для первых двух реакций, приводящих к одному и тому же составному ядру - ^{205}At , получены данные о значениях сечений каналов ($4n \div 9n$) и (p, $5n \div 9n$) в области энергий возбуждения составного ядра от 55 МэВ до 135 МэВ. В реакциях с ионами ^{40}Ca измерены сечения для каналов $3n$, (p, $2n \div p$, $4n$). Проведено сравнение результатов с модельными расчетами, выполненными по модифицированной программе ALICE. Показано, что несмотря на большой диапазон изменения величин сечений и необходимость одновременного описания двух типов каналов, удается получить неплохое согласие расчета с экспериментом для реакций $^{165}\text{Ho} + ^{40}\text{Ar}$ и $^{181}\text{Ta} + ^{24}\text{Mg}$. Для реакции $^{159}\text{Tb} + ^{40}\text{Ca}$ расчетные значения сечений превышают экспериментальные данные на порядок. Обсуждаются возможные причины такого расхождения.

Работа выполнена в Лаборатории ядерных реакций ОИЯИ.

Препринт Объединенного института ядерных исследований. Дубна 1989

Andreyev A.N. et al. Е7-89-809
Production Cross Sections of Neutron Deficient Isotopes
of At and Po from Nuclear Reactions
 $^{165}\text{Ho} + ^{40}\text{Ar}$, $^{159}\text{Tb} + ^{40}\text{Ca}$ and $^{181}\text{Ta} + ^{24}\text{Mg}$

Experiments have been carried out to measure the xn and pxn channels cross sections in the reactions $^{165}\text{Ho} + ^{40}\text{Ar}$, $^{181}\text{Ta} + ^{24}\text{Mg}$ and $^{159}\text{Tb} + ^{40}\text{Ca}$. For the first two reactions leading to the same compound nucleus, ^{205}At , data on the cross sections of the $4n \div 9n$ and $p5n \div p9n$ channels have been obtained for the compound nucleus excitation energies ranging from 55 MeV to 135 MeV. In the reaction induced by the ^{40}Ca ions the cross sections of the $3n$, $p2n \div p4n$ channels have been measured. The results obtained are compared with the model calculations using modified program ALICE. It is shown that the calculated results agree with experimental ones fairly well for the reactions $^{165}\text{Ho} + ^{40}\text{Ar}$ and $^{181}\text{Ta} + ^{24}\text{Mg}$ despite widely varying cross section values and the necessity to describe the two channels simultaneously. For the reaction $^{159}\text{Tb} + ^{40}\text{Ca}$ the calculated cross sections are one order of magnitude larger than the experimental ones. The possible reasons for this discrepancy are discussed.

The investigation has been performed at the Laboratory of Nuclear Reactions, JINR, Preprint of the Joint Institute for Nuclear Research, Dubna 1989